THE ROLE OF EVOLUTIONARY AGE AND METALLICITY IN THE FORMATION OF CLASSICAL BE CIRCUMSTELLAR DISKS II. ASSESSING THE TRUE NATURE OF CANDIDATE DISK SYSTEMS

J.P. Wisniewski[1,2,3], K.S. Bjorkman[3,4], A.M. Magalhães[3,5], J.E. Bjorkman[4], M.R. Meade[6], & Antonio Pereyra[5]

Draft version November 27, 2006

ABSTRACT

Photometric 2-color diagram (2-CD) surveys of young cluster populations have been used to identify populations of B-type stars exhibiting excess Hα emission. The prevalence of these excess emitters, assumed to be "Be stars", has led to the establishment of links between the onset of disk formation in classical Be stars and cluster age and/or metallicity. We have obtained imaging polarization observations of six SMC and six LMC clusters whose candidate Be populations had been previously identified via 2-CDs. The *interstellar* polarization (ISP) associated with these data has been identified to facilitate an examination of the circumstellar environments of these candidate Be stars via their intrinsic polarization signatures, hence determine the true nature of these objects. We determined that the ISP associated with the SMC cluster NGC 330 was characterized by a modified Serkowski law with a λ_{max} of $\sim$4500Å, indicating the presence of smaller than average dust grains. The morphology of the ISP associated with the LMC cluster NGC 2100 suggests that its interstellar environment is characterized by a complex magnetic field.

Our *intrinsic* polarization results confirm the suggestion of Wisniewski et al. that a substantial number of bona-fide classical Be stars are present in clusters of age 5-8 Myr. Hence, our data contradict recent assertions that the Be phenomenon develops in the second half of a B star's main sequence lifetime, i.e. no earlier than 10 Myr. These data imply that a significant number of B-type stars must emerge onto the zero-age-main-sequence rotating at near-critical rotation rates, although we can not rule out the possibility that these data instead reveal the presence of a sub-group of the Be phenomenon characterized by sub-critically rotating objects. Comparing the polarimetric properties of our dataset to a similar survey of Galactic classical Be stars, we find that the prevalence of polarimetric Balmer jump signatures decreases with metallicity. We speculate that these results might indicate that either it is more difficult to form large disk systems in low metallicity environments, or that the average disk temperature is higher in these low metallicity environments. We have characterized the polarimetric signatures of all candidate Be stars in our data sample and find $\sim$25% are unlikely to arise from true classical Be star-disk systems. This detection of such a substantial number "contaminants" suggests one should proceed with caution when attempting to determine the role of evolutionary age and/or metallicity in the Be phenomenon purely via 2-CD results.

Subject headings: Magellanic Clouds — stars: emission-line, Be — circumstellar matter — techniques: polarimetric — clusters:individual (Bruck 60, NGC 330, NGC 346, NGC 371, NGC 456, NGC 458, LH 72, NGC 1818, NGC 1858, NGC 1948, NGC 2004, NGC 2100) — stars:individual (pi-Aquarii)

1. INTRODUCTION

While the rapid rotation (v_{eq}/v_{crit} $\sim$70-80% of their critical velocity; Porter 1996; Porter & Rivinius 2003) of classical Be stars has long been speculated to be the fundamental source driving the production their geometrically thin circumstellar disks (Struve 1931; Porter & Rivinius 2003), recent photometric surveys (Feast 1972; Grebel, Richtler, & de Boer 1992; Grebel 1997; Dieball & Grebel 1998; Keller et al. 1999; Grebel & Chu 2000; Keller et al. 2000; Olsen et al. 2001; McSwain & Gies 2005; Wisniewski & Bjorkman 2006) have suggested secondary mechanisms might contribute to the observed phenomenon. Specifically, Mermilliod (1982); Grebel (1997); Fabregat & Torrejon (2000); Keller (2004) found that the frequency of the Be phenomenon seems to peak in clusters with a main sequence turn-off of B1-B2, leading to the suggestion that the Be phenomenon is enhanced with evolutionary age. Several recent observational studies (Grebel, Richtler, & de Boer 1992; Mazzali et al. 1996; Grebel 1997; Maeder, Grebel, & Mermilliod 1999; Keller 2004) have also suggested that the Be phenomenon may be more prevalent in low metallicity environments, based on comparisons of the fractional Be populations of Galactic, LMC, and SMC clusters.

[1] NPP Fellow

[2] NASA Goddard Space Flight Center, Code 667, Greenbelt, MD 20771 USA jwisnie@milkyway.gsfc.nasa.gov

[3] Visiting Astronomer, Cerro Tololo Inter-American Observatory

[4] Department of Physics and Astronomy MS 113, University of Toledo, Toledo, OH 43606-3390 USA, karen@physics.utoledo.edu, jon@physics.utoledo.edu

[5] IAG, Universidade de São Paulo, Caixa Postal 3386, São Paulo, SP 01060-970, Brazil, mario@astro.iag.usp.br, antonio@astro.iag.usp.br

[6] Space Astronomy Lab, University of Wisconsin-Madison, 1150 University Avenue, Madison, WI 53706 USA, meade@sal.wisc.edu

In Wisniewski & Bjorkman (2006) (hereafter WB06), we used a simple 2-color diagram (2-CD) technique to identify the fractional candidate Be population of numerous Large Magellanic Cloud (LMC), Small Magellanic Cloud (SMC), and Galactic clusters in an effort to improve the statistical database which has been used to link classical Be disk formation with evolutionary age and/or metallicity. WB06 found compelling evidence that the Be phenomenon develops much earlier than previously predicted by theory (Fabregat & Torrejon 2000), i.e before the mid-point main sequence lifetime; furthermore, they found evidence of an additional enhancement in the fractional Be content of clusters with evolutionary age. The increased statistics offered by this work, while confirming the previously suggested trend of an enhancement in the Be phenomenon in low metallicity environments, lowered the average fractional Be content of SMC clusters from 39% (Maeder, Grebel, & Mermilliod 1999) to 32%.

While the 2-CD has been widely used to link evolutionary age and/or metallicity with Be disk formation, it is inherently unclear whether all B-type objects identified as excess Hα emitters, i.e. "Be stars", are truly classical Be stars. It has been noted that other B-type objects, such as Herbig Ae/Be stars, post-main-sequence B[e] stars, and supergiants, may also exhibit Hα emission hence "contaminate" these claimed detections (WB06).

Polarimetry is a tool which has long been used to investigate the circumstellar environments of Be stars (Coyne & Kruszewski 1969; Poeckert & Marlborough 1976; Coyne & McLean 1982; Bjorkman 1994; McDavid 1994; Quirrenbach et al. 1997; Wood, Bjorkman, & Bjorkman 1997; Clarke & Bjorkman 1998). Electron scattering in the innermost region of classical Be circumstellar disks will polarize a small fraction of stellar photons; furthermore, pre- and post-scattering attenuation by hydrogen atoms within the inner disk region will imprint a characteristic wavelength dependence onto this polarization signature if the inner disk is sufficiently dense (Wood & Bjorkman 1995). The wavelength dependence of polarization originating from classical Be stars, characterized by geometrically thin, gaseous circumstellar disks, (Quirrenbach et al. 1997; Wood, Bjorkman, & Bjorkman 1997; Clarke & Bjorkman 1998) is significantly different than that expected from the dustier circumstellar environments of Herbig Ae/Be stars, post-main-sequence B[e] stars, and supergiants. Thus for non-pole-on disk geometries, polarimetry can be employed to investigate circumstellar environments and discriminate the evolutionary nature of sources.

In this paper, we use imaging polarimetry to investigate the true nature of candidate Be stars in six LMC and six SMC clusters which were initially identified via photometric 2-CDs. In Section 2, we outline our observations and data reduction techniques. In Section 3, we detail how we identified and removed the interstellar polarization component associated with each of our lines of sight. We develop a classification system to characterize the intrinsic polarization observed in our candidate Be star sample in Section 4 and also discuss the results of individual clusters. We discuss the implications of these results in Section 5 and summarize our work in Section 6.

2. OBSERVATIONS AND DATA REDUCTION

The imaging polarimetry data presented in this study were obtained at the CTIO 1.5m. The F/7.5 secondary configuration was used during our 2001 observing run, which yielded a 15 x 15 arc-minute field of view and a 0.44 arc-second pixel^{-1} scale, while the F/13.5 secondary configuration, which provided a 8 x 8 arc-minute field of view with a 0.24 arc-second pixel^{-1} scale, was used during our 2002 observing run. Data were recorded with CTIO's standard Cassegrain focus CCD (CFCCD), a 2048 x 2048 multi-amplifier CCD. The standard CFCCD configuration was modified by the addition of a rotatable half-wave plate followed by a fixed analyzer, the latter of which was placed in the upper of the 1.5m's two filter wheels. The polymer achromatic wave-plate was manufactured by Meadowlark Optics and provided polarization modulation for each 90° rotation of the wave-plate. Unless otherwise noted, each of our fields of view was observed with the wave-plate rotated through 8 positions 22.5° apart. The fixed analyzer was a double calcite block whose optical axes had been crossed to minimize astigmatism and color effects. Further details about this polarimeter can be found in Magalhães et al. (1996), Pereyra (2000), Melgarejo et al. (2001), & Pereyra & Magalhães (2002). We placed CTIO's Tek U, B, V, R, and I filters in the second filter wheel. A summary of the science clusters we observed is presented in Table 1.

Nightly observations of polarization standard stars were obtained to calibrate the polarimetric efficiency of each filter and determine the zero-point of the polarization position angle in each filter, while nightly observations of unpolarized standard stars were obtained to characterize any instrumental polarization present. Our unpolarized standard data indicate that the polarimeter had an instrumental polarization consistent with zero for our 2001 data. The B, V, R, and I filters of our 2002 data also had an instrumental polarization consistent with zero (Wisniewski et al. 2003), while the U filter data had an instrumental polarization of $\sim$0.1%, which was removed from the data.

The reduction of these data began with standard image processing, including bias and flat field corrections, using standard IRAF[7] techniques. Following this initial processing, aperture photometry was performed for all point sources in each of the 8 images of an observation set, using 10 apertures of size 3-12 pixels for the F/7.5 data and 5-14 pixels for the F/13.5 data. The linear polarization of each source was extracted from a least squares solution of the difference amplitudes in the 8 wave-plate positions (ψ_i), using the PCCDPACK software suite (Pereyra 2000; Pereyra & Magalhães 2002). Both the expected photon noise errors and the actual measured errors, defined as the residuals at each wave-plate position with respect to the expected $\cos 4\psi_i$ curve, were also calculated. With few exceptions, these two errors were consistent with one another.

3. INTERSTELLAR POLARIZATION

The polarization observed in our raw data is comprised of the superposition of an interstellar component, attributable to the dichroic absorption of starlight by partially aligned dust grains along each line of sight, and an in-

[7] IRAF is distributed by the National Optical Astronomy Observatories, which are operated by the Association of Universities for Research in Astronomy, Inc., under contract with the National Science Foundation.

trinsic component, originating from the host star's circumstellar environment. As most of the objects in our fields of view should be normal main sequence stars lacking any type of asymmetrical circumstellar envelope, they should not exhibit an intrinsic polarization component. Furthermore, we can assume that all stars in our fields of view are located at the same general distance, since they are members of a cluster population, and that the properties of the interstellar medium do not significantly vary over the angular extent of our clusters. Hence each cluster in our sample provides us with a multitude of suitable "field stars" whose polarization we can simply average to estimate the interstellar polarization (ISP) along each line of sight, via the commonly used field star technique (McLean & Brown 1978).

In Figure 1 we show the total V-band polarization of all sources in the LMC cluster NGC 1818 having polarimetric signal-to-noise ratios (p/σ_p) greater than 5.0. The distinctive grouping of most objects in the Stokes Q-U diagram of this figure (panel a) and the narrow polarization (panel d) and position angle (panel c) histograms demonstrates that most of these objects do lack significant intrinsic polarization components and only have an ISP component. After excluding objects outside of the dominant trends found in these histograms with an iterative method, we calculated the weighted average and standard deviation of these data to determine a preliminary estimate of this cluster's V-band ISP, as shown in Figure 2. The wavelength dependence of these estimates clearly follow the empirical Serkowski law (Serkowski et al. 1975) commonly used to parameterize an ISP. Over-plotted in Figure 2 is a modified Serkowski law (Serkowski et al. 1975; Wilking et al. 1982) which we deemed best represented the observational data. The polarization at the midpoint wavelength location of the U, B, V, R, and I filters was then extracted from this curve and served as the final estimate of the ISP. The modified Serkowski parameters determined for all of our lines of sight, along with the extracted filter ISP values, are summarized in Table 2.

The ISP values compiled in Table 2 are relevant to our efforts to isolate the intrinsic polarization components associated with our target stars; however, they do not yet yield any direct information regarding the properties of the interstellar dust grains which reside in their parent LMC and SMC clusters, as these ISP values are comprised of both foreground Galactic ISP and Magellanic Cloud ISP contributions. Following the techniques used by Clayton et al. (1983) and Rodrigues et al. (1997), we used the interstellar polarization maps of Schmidt (1976), to identify and remove this foreground Galactic ISP contribution (see Table 3), hence determine estimates of the ISP intrinsic to our LMC and SMC clusters (see Table 4). We used a modified Serkowski-law (Serkowski et al. 1975; Wilking et al. 1982) to extrapolate these maps over the wavelength range of our dataset, and assumed a nominal Galactic λ_{max} value of 5500Å to characterize the parameter K. The errors cited in the Galactic polarization maps (Schmidt 1976) and those present in our total ISP estimates (Table 2) were propagated to produce the error estimates cited in Table 4.

Most of the field stars used to derive our total ISP estimates were not highly reddened objects, hence the intrinsic LMC and SMC ISP values listed in Table 4 all are characterized by modest polarization amplitudes, which are often on the order of the errors of our data. In spite of this fact, numerous trends in these data are clearly present. As expected, the magnitude of UBVRI polarization towards each cluster follows a Serkowski-like wavelength dependence at a wavelength independent position angle. This lack of position angle rotation indicates that our Galactic interstellar polarization correction was reasonable and that we are looking at a single magnetic field orientation towards each of our clusters. All LMC clusters exhibit similar ISP properties, with polarization magnitudes ranging from ~0.2-0.5% at a position angle of ~25-45 degrees; similarly, all SMC clusters also exhibit clear evidence of sharing common ISP properties, with polarization magnitudes ranging from ~0.3-0.6% at a position angle of ~120-150 degrees. The shallow curvature of the Serkowski-law dependence of these data, in combination with the moderate level of uncertainty present, make identifying systematic differences in the interstellar dust grain properties of these clusters difficult. The total ISP (Table 2) and SMC ISP (Table 4) of the cluster NGC 330 does however show suggestive evidence of being characterized by a short wavelength λ_{max} value of ~4500 Å (Figure 3). Such an effect is commonly attributed to the presence of small dust grains, and has been previously observed in other SMC sight-lines (Rodrigues et al. 1997). In a future paper, we will examine the wavelength dependence of highly reddened and moderately reddened objects in our dataset, observed at high signal-to-noise, to perform a more detailed investigation of the interstellar medium properties of these LMC and SMC clusters.

3.1. *NGC 2100*

The total polarization vectors of our observations of the LMC cluster NGC 2100 clearly exhibit evidence of a collective, complex morphology (see Figure 4). While Figure 4 only presents I-band data, all of our other filters exhibit similar alignment patterns. Recall that we expect most cluster objects should not exhibit an intrinsic polarization component; thus we suggest that these systematic morphological changes are related to changes in the magnetic field properties within our field of view. A substantial discussion of the magnetic field properties of NGC 2100 is presented in Wisniewski et al. (2006). For the purposes of the present study, we will only discuss our efforts to parameterize and remove the ISP along the line of sight to this cluster.

We identified three spatial regions in our field of view, corresponding to the region around the cluster core, the region to the south of the cluster core, and the region to the north of the core, which displayed unique ISP characteristics. In Figures 5, 6, and 7, we show the B-band polarization vector maps of what we have defined as regions 1, 2, and 3 respectively in the total ISP along the line of sight to NGC 2100, overlaid on DSS-2 blue images. Having identified these distinct regions, we then extracted total ISP estimates following the technique previously described. We calculated a σ^{-2} weighted average of all objects in each filter served as an initial ISP estimate, determined the modified Serkowski-law parameters which best represented the data, as seen in Figure 8 for region 1, and

extracted final ISP values (Table 5) for each region from these Serkowski curves. The locations of the candidate Be stars in NGC 2100 were then correlated to these 3 ISP regions to determine the ISP correction each should receive. We found NGC 2100:KWBBe 102, 630, and 712 resided in area 2, NGC 2100:KWBBe 535, 797, and 1033 resided in area 3, and the rest of the candidate Be stars resided in area 1.

4. INTRINSIC POLARIZATION

We subtracted the ISP from the observed polarization to isolate any intrinsic polarization components present. The location of candidate Be stars in our fields of view were identified by careful correlation with literature coordinates and finder charts. Using several PCCDPACK routines, we meticulously examined the extracted polarization for each of the candidate Be stars in our sample to search for undesired contamination by a) the ordinary or extraordinary images of nearby objects and b) cosmic ray hits or uncorrected bad pixels. The total polarization of all candidate Be stars which did not suffer from these contamination issues are tabulated in Table 6, while the intrinsic polarization of these objects are tabulated in Table 7.

Recall from the introduction that electron scattering events in non-pole-on classical Be stars will produce a wavelength independent polarization magnitude and position angle signal. Furthermore, pre- or post-scattering absorption will superimpose the wavelength dependent signature of hydrogen opacity on this signal, creating a "sawtooth" polarization signature (Bjorkman 2000) if enough absorption events occur. Examples of these two signatures of classical Be circumstellar disks are given in Figure 9, which presents multi-epoch observations of the known classical Be star pi Aquarii as observed by the University of Wisconsin's HPOL spectropolarimeter. We have contemporaneously analyzed the Stokes Q-U diagrams of all candidate Be stars' total and intrinsic polarization components to search for evidence of these signatures, i.e. evidence that they are true classical Be star-disk systems, and have developed a conservative 4-point classification scale to rank the likelihood that they are classical Be stars. Results of this classification are summarized in Table 8 for individual objects and in Table 9 for the net results of entire clusters. The design of our classification system emphasized the identification of both objects which were bona-fide classical Be stars and objects which were clearly unlikely to be classical Be stars. Specifically, we defined our classification system by:

- **Type-1:** Objects which are *definitely* classical Be stars;
- **Type-2:** Objects whose polarimetric properties are *not inconsistent* with those expected from classical Be stars;
- **Type-3:** Objects which are *unlikely* to be classical Be stars; and
- **Type-4:** Objects which are *highly unlikely* to be classical Be stars.

Stars in our sample which displayed, to within 3 σ, a "sawtooth-like" polarization Balmer jump (BJ) along with a wavelength independent polarization position angle (see Figure 10) were assigned a designation of type-1. We claim that all type-1 objects are definitely classical Be stars.

We assigned a designation of type-2 to objects whose polarimetric properties were not inconsistent with that expected from a classical Be star-disk system. As previously discussed, classical Be disks of sufficiently low density will not leave an imprint of hydrogen opacity in their intrinsic polarization signals; hence, stars which exhibited, to within 3σ, a wavelength independent electron scattering (ES) polarization signature (see Figure 11) received a designation of type-2. A small number of objects exhibited a nearly wavelength independent polarization magnitude along with a minor wavelength dependence in their polarization position angles; we designated these objects as type-2 as we believe such stars most likely are exhibiting ES signatures modified by a slight under- or over-correction of their ISP components. We can not rule out that this minor wavelength dependence might also be produced by the additional presence of an optically thin dust disk, as present in post-main-sequence B[e] stars (Magalhães 1992; Melgarejo et al. 2001). Finally, we assigned all objects which appeared to be intrinsically unpolarized ($< 0.3\%$ polarization), to within 3σ, a type-2 designation as this is the expected signature of pole-on or nearly pole-on classical Be stars. We caution the reader that we are not 100% certain that these unpolarized objects are classical Be stars as: a) stars without gaseous disks, spuriously detected as excess Hα emitters on 2-CDs, will also exhibit zero net intrinsic polarization and b) the noise present in the observations of fainter targets may preclude us from clearly identifying them as "contaminants".

We assigned the designation of type-3 to type-4 to objects whose polarization, to within 3σ, appeared to be inconsistent with the aforementioned signatures expected from a classical Be star-disk system (see e.g. Figure 12). We briefly discuss some of the major types of atypical polarimetric signatures we observed.

In Table 8, we assigned a designation of type 3-4 to several objects whose intrinsic polarization exhibited signs of a 90° position angle reversal (Figure 14), which is a signature of a dusty bipolar nebula geometry (Schmidt et al. 1992; Schulte-Ladbeck et al. 1992). From an inspection of the Stokes Q-U diagram of such an object (Figure 14), it is clear that even if our initial ISP correction was grossly miscalculated, the wavelength dependent polarization would still be inconsistent with that expected from classical Be stars. While it would be interesting to further probe the circumstellar environments of such objects with follow-up investigations, for the purposes of this paper we merely remark that they are unlikely to be classical Be stars.

Several of our candidate Be stars exhibited very large (1-3.5%), complex intrinsic polarization signatures (see Figure 13). Given the steep drop in their polarization magnitude at short optical wavelengths, along with subtle indications of a corresponding position angle rotation, it is possible that these objects are characterized by dusty bipolar nebulae whose polarization signature exhibits a position angle reversal at UV wavelengths, similar to HD 45677 (Schulte-Ladbeck et al. 1992). Alternatively, the polariza-

tion of these objects could be interpreted as following a Serkowski-like wavelength dependence characterized by a large λ_{max} value. As our data have already been corrected for the average ISP associated with each of our clusters, this latter interpretation would require these objects to be situated in region of patchy dust, likely populated by larger grains given the long wavelength values of λ_{max}, i.e. $>$ 7000 Å in Figure 13 (Rodrigues et al. 1997; Whittet et al. 1992). Serkowski et al. (1975) described the expected magnitude of interstellar polarization by the formulation $3E_{B-V} \leq P_{max} \leq 9E_{B-V}$; hence, an additional reddening of 0.3 - 1.0 E($B-V$ would be required to produce the measured p_{max} of these objects, ~3%. The observed colors of at least some of these objects (NGC 1948:KWBBe 98, V-I = 0.67; Keller et al. 1999) is likely sufficient to produce the amount of purported additional ISP, although other objects (NGC 1948:KWBBe 246, V-I = 0.05; Keller et al. 1999) clearly do not meet this criteria. While follow-up optical or infrared spectroscopy of these annomalous candidates would help to determine whether they exhibit a dusty bipolar nebula geometry or are located in a region of patchy dust, for the purpose of this paper we merely stress that it is clear that these objects are not likely to be classical Be stars.

We now offer discussion of the polarimetric properties of candidate Be stars in individual clusters. Recall that all candidates which exhibited evidence of contamination, predominantly from nearby neighbors, have been excluded from our analysis. We further note that the effective limiting magnitude of our polarimetric dataset was lower (i.e. brighter) than that considered in WB06.

4.1. *LMC Clusters*

4.1.1. *NGC 1818*

Keller et al. (1999) identified 40 candidate Be stars associated with the LMC cluster NGC 1818 and its surrounding field. The cluster is densely populated, and because of image overlap issues, we were only able to retrieve polarimetric information for 18 of these candidate Be stars. 4 of these 18 (22%) showed intrinsic polarization Balmer jump (BJ) signatures, NGC 1818:KWBBe 69, 82, 137, 243. We classified 12 of the 18 candidates (67%) as type-2 objects, and found 5 of the type-2 objects (i.e. 5 of the 18 stars, 28%, in the total population) exhibited clear evidence of an electron scattering (ES) polarization signature. 2 of the 18 candidates (11%), NGC 1818:KWBBe 47 and 381, were deemed unlikely to be classical Be stars. While the B, V, R, and I filter polarization of NGC 1818:KWBBe 47 were consistent with an ES signature, the U filter exhibited a significant position angle rotation which was inconsistent with an ES origin. Although noisy, the observation of NGC 1818:KWBBe 381 also did not follow an ES wavelength dependence, prompting us to assign it an "unlikely Be star" designation.

4.1.2. *NGC 1948*

Keller et al. (1999) identified 27 candidate Be stars associated with the cluster NGC 1948 and its nearby field. We were able to extract polarimetric information on 22 of these candidates from our data set. 6 of these 22 candidates (27%) exhibited a polarization Balmer jump, NGC 1948:KWBBe 71, 75, 102, 153, 172, and 240. We classified 12 of the 22 candidates (55%) as type-2 objects, and found 6 of the type-2 objects (i.e. 6 of the 22, 27%, in the total population) exhibited a definite electron scattering polarization signature, NGC 1948:KWBBe 62, 92, 101, 157, 326, and 790. We note that NGC 1948:KWBBe 92 does show a hint of a small polarization Balmer jump; however, we opted to describe its polarization more conservatively, i.e. as having an electron scattering signature. We found 4 of the 22 stars (18%) had polarimetric properties which suggested that they were unlikely to be classical Be stars. As previously discussed, 3 of these stars, NGC 1948:KWBBe 98, 183, and 246 exhibited intrinsic polarization signals which seemed to follow a Serkowski-like wavelength dependence. NGC 1948:KWBBe 91 was also deemed unlikely to be a classical Be star due to the wavelength dependent nature of its polarization position angle.

4.1.3. *NGC 2004*

Keller et al. (1999) identified 67 candidate Be stars associated with the LMC cluster NGC 2004 and its surrounding field. We extracted polarimetric information for 43 of these candidates, and found that 9 of the 43 (21%), namely NGC 2004:KWBBe 50, 87, 96, 103, 106, 152, 211, 347, 377, showed an intrinsic polarization Balmer jump. 28 of the 43 candidates (65%) were classified as type-2 objects, and note that 10 of these 28 type-2 objects (i.e. 10 of the 43, 23%, in the total population), NGC 2004:KWBBe 91, 203, 276, 323, 344, 441, 624, 717, 1175, and 1421 exhibited an electron scattering polarization signature. We found 6 of the 43 (14%) candidates in NGC 2004 were unlikely to be classical Be stars based on their intrinsic polarization. Of these objects, we note that the 3 filters of polarization extracted for NGC 2004:KWBBe 1315 show suggestive evidence of a polarization position angle flip, a feature which is not expected in classical Be star-disk systems.

4.1.4. *LH 72*

WB06 identified 50 candidate Be stars in the LMC cluster LH 72, and designated 11 of these detections as tentative. We were able to obtain polarimetric information for 34 of these stars: 1 of the 34 (3%), LH 72:WBBe 5, showed a polarization Balmer jump and thus should be considered a bona-fide classical Be star. We classified 22 of the 34 (65%) stars as type-2 objects, and found 5 of these 22 type-2 objects (i.e. 5 of the 34, 15%, of the total population), LH 72:WBBe 13, 15, 26, 27, and 33 exhibited an electron scattering polarization signature. We suggest that 11 of the 34 (32%) of candidates in LH 72 are unlikely to be classical Be stars based on their intrinsic polarization properties. Of these unlikely Be stars, we found that the intrinsic polarization of LH 72:WBBe 9 followed a Serkowski-like wavelength dependence, with a λ_{max} value $>$ 6000 Å. We extracted polarimetric information for 7 of the 11 stars designated as possible candidate Be stars by WB06. 5 of these 7 stars were classified as type-2 objects, while 2 of the 7 appear unlikely to be classical Be stars based on their intrinsic polarization signatures.

4.1.5. *NGC 1858*

WB06 identified 39 candidate Be stars in the LMC cluster NGC 1858, and we were able to extract polarimetric information for 27 of these 39 stars. 3 of the 27 (11%), NGC 1858:WBBe 6, 9, and 20, exhibited polarization Balmer jumps. We classified 13 of the 27 (48%) as type-2 objects, and found 2 of these 13 type-2 stars (i.e. 2 of the 27, 7%, of the total population) exhibited an electron scattering polarization signature. 11 of the 27 (41%) candidates in NGC 1858 appear unlikely to be classical Be stars based on their polarimetric signatures. As previously discussed, 2 of these unlikely Be stars, NGC 1858:WBBe 3 and 12 had an intrinsic polarization which follow a Serkowski-like wavelength dependence, characterized by a long λ_{max} value. 4 of the 39 photometrically identified candidate Be stars in NGC 1858 were judged to be possible detections in WB06: we were able to detect 3 of these 4 polarimetrically. We classified 2 of the 3 to be type-2 objects, and the remaining object, NGC 1858:WBBe 9, as a type-1 object.

4.1.6. *NGC 2100*

Keller et al. (1999) identified 61 candidate Be stars associated with the LMC cluster NGC 2100. We were able to extract polarimetric information for 35 of the 61 candidates (57%). 8 of the 35 stars (23%), NGC 2100:KWBBe 79, 97, 436, 619, 635, 705, 770, and 797, exhibited polarization Balmer jumps and hence are definitely classical Be stars. 20 of the 35 stars (57%) were classified as type-2 stars, and we found 16 of these 20 type-2 stars (i.e. 16 of the 35, 46%, of the total population) exhibited an electron scattering intrinsic polarization signature. We suggest that 7 of the 35 (20%) candidates in NGC 2100 are unlikely to be classical Be stars based on their observed intrinsic polarization signatures. Note that the intrinsic polarization of NGC 2100:KWBBe 321 seems to follow a Serkowski-like wavelength dependence, while the unique intrinsic polarization signatures of NGC 2100:KWBBe 111 and 219 (Figure 14) suggests these objects might be dust-disk systems.

4.2. *SMC Clusters*

4.2.1. *NGC 346*

Keller et al. (1999) identified 48 candidate Be stars in the vicinity of the SMC cluster NGC 346: we have obtained polarimetric information for 33 of these objects. 8 of the 33 objects (24%), NGC 346:WBBe 85, 93, 191, 236, 374, 445, 468, and 529, exhibited polarization Balmer jumps and hence are definitely classical Be stars. We classified 22 of the 33 stars (67%) as type-2 stars, and found 7 of these 22 type-2 objects (i.e. 7 of the 33, 21%, of the total population) exhibited a clear electron scattering intrinsic polarization signature. We suggest that 3 of the 33 candidates in NGC 346 (9%) are unlikely to be classical Be stars based on their polarimetric signatures.

4.2.2. *NGC 371*

WB06 identified 129 candidate Be stars in NGC 371. We have obtained polarimetric information for 73 of these targets, and found 10 of these 73 stars (14%), NGC 371:WBBe 2, 3, 4, 5, 6, 10, 13, 18, 24, and 31 exhibited polarization Balmer jumps, indicating they are definitely classical Be stars. We classified 49 of the 73 stars (67%) as type-2 objects, and remark that 6 of these 49 type-2 stars (i.e. 6 of the 73, 8%, of the total population) exhibited a clear electron scattering polarization signature. Note that many of the fainter candidate Be stars included in our 74 detections were not observed at high signal-to-noise levels; thus for most of these objects we can only say that to within 3σ, their polarimetric properties are not inconsistent with those of classical Be stars. We suggest that 14 of the 73 (19%) candidates in NGC 371 are unlikely to be classical Be stars based on their polarimetric properties. WB06 suggested that 11 of the 130 photometrically identified candidates should be viewed as "possible detections"; however, we were only able to extract polarimetric information for 2 of these 11 objects, NGC 371:WBBe 64 and 87. We classified both as type-2 stars.

4.2.3. *Bruck 60*

We were able to extract polarimetric information for 18 of the 60 candidate Be stars identified photometrically by WB06. We found 1 of the 18 (6%), Bruck 60:WBBe 6, showed a polarization Balmer jump, while we classified 11 of the 18 stars (61%) as type-2 objects. 8 of these 11 type-2 stars (i.e. 8 of the 18, 44%, of the total population) exhibited an electron scattering intrinsic polarization signature. We suggest that 6 of the 18 (33%) candidates in Bruck 60 are unlikely to be classical Be stars based on their polarimetric signatures. WB06 noted that 5 of the 26 photometrically identified candidate Be stars in Bruck 60 should be considered "possible detections". We were only able to detect 1 of these 5 stars polarimetrically, Bruck 60:WBBe 21, and classified it as a type-2 object which exhibited clear evidence of an electron scattering polarization signature.

4.2.4. *NGC 456*

23 candidate Be stars in NGC 456 were identified in the photometric survey of WB06, and we were able to extract polarimetric information for 14 of these 23 candidates. Although we did not observe any objects with polarimetric Balmer jumps, we did classify 9 of the 14 stars (64%) as type-2 objects. 1 of these 9 type-2 stars (i.e. 1 of the 14, 7%, of the total population), NGC 456:WBBe 1, exhibited an electron scattering polarization signature. We suggest that 5 of the 14 (36%) candidates in NGC 456 are unlikely to be classical Be stars based on their observed intrinsic polarization components. WB06 suggested 1 of NGC 456's 23 photometrically identified candidate Be stars should be viewed as a "possible detection": we marginally detected this object, NGC 456:WBBe 21, and suggest that it is unlikely to be a classical Be star.

4.2.5. *NGC 458*

30 candidate Be stars were photometrically identified in NGC 458 by WB06, and we were able to extract polarimetric information for 10 of these 30 candidates. None of the 10 detected objects exhibited polarimetric Balmer jumps or clear evidence of having an electron scattering signature. We classified 6 of the 10 stars (60%), and suggest that 4 of the 10 (40%) are unlikely to be classical Be stars. We were able to extract polarimetric information for 1 of the 2 initially identified as "possible detections" by WB06, NGC 458:WBBe19. We classified this

star as a type-2 object; furthermore, we found it exhibited suggestive evidence of a small polarimetric Balmer jump, although the data were very noisy.

4.2.6. *NGC 330*

Keller et al. (1999) identified 76 candidate Be stars in the vicinity of NGC 330 and we were able to extract polarimetric information for 41 of these objects. While we did not observe any of the detected candidates to have a polarimetric Balmer jump, we did classify 24 of the 41 (59%) candidates as type-2 stars, and note that 9 of these 24 type-2 objects (i.e. 9 of the 41, 22%, of the total population) exhibited electron scattering polarimetric signatures. We suggest that 17 of the 41 (41%) candidates are unlikely to be classical Be stars based on their intrinsic polarimetric signatures.

5. DISCUSSION

5.1. *Analysis of Intrinsic Polarization Statistics*

It is clear from Table 9 that the percentage of SMC and LMC candidate Be stars which exhibit polarization Balmer jumps, electron scattering signatures, or were deemed unlikely to be classical Be stars varies significantly from one cluster to the next. To better assess the global trends of our dataset, we extracted simple statistical mean and median values from Table 9, as summarized in Table 10. From Table 10, we see that at least 25% of our dataset is populated by objects which appear unlikely to be classical Be stars. The presence of such a large number of likely "contaminants" is interesting, as it confirms one of the initial hypotheses of this project: it is dangerous to assume, a-priori, that all objects identified as excess Hα emitters via 2-CD surveys are classical Be stars. We thus suggest caution should be exercised when attempting to ascertain the role evolutionary age and/or metallicity play in the development of the Be phenomenon purely via the analysis of 2-CD data.

Assuming these objects are truly "contaminants", we recalculated the statistics of our intrinsic polarization dataset after removing these objects from consideration. The results of this exercise are listed in Table 11. The median prevalence of polarization Balmer jumps in our SMC/LMC dataset is typically between 20-25% (Table 11). Polarization Balmer jumps appear to be significantly less prevalent in our SMC clusters (4%) than in our LMC clusters (25%); however, this statistic is strongly influenced by the null detection of such signatures in three SMC clusters.

Since 1989, the HPOL spectropolarimeter (Wolff et al. 1996) mounted on the University of Wisconsin's Pine Bluff Observatory (PBO) has been monitoring the optical spectropolarimetric properties of a sample of 73 known Galactic Be stars, and it provides a statistically significant polarimetric dataset which we will use to aid the interpretation of our results. As yet, most of the ~800 HPOL observations of classical Be stars have not had their ISP components identified and removed; hence, we can not readily compare their intrinsic polarization characteristics to our data. However, we can determine the prevalence of polarization Balmer jumps in the HPOL database. Data obtained prior to 1995 have been compiled in catalog form by Bjorkman et al. (2000), and observations characterized by a polarization Balmer jump have already been flagged in the catalog. We have similarly analyzed all observations obtained from 1995-2004 to identify the presence of polarimetric Balmer jumps in these data. We then compiled all HPOL observations of individual classical Be stars into two categories: a) classical Be stars which had **never** exhibited a polarimetric Balmer jump in any PBO observation; and b) classical Be stars which had exhibited a polarimetric Balmer jump in at least one observation. The results of this classification procedure are given in Table 11.

We found 31 of the 73 (42%) observed Galactic Be stars exhibited a polarimetric Balmer jump for at least part of the time-frame of the HPOL survey. Amongst early-type Be stars (O9-B5) in the HPOL database, 22 of 45 (49%) exhibited polarimetric Balmer jumps. Note that further restricting the sample to include only O9-B3 type Be stars does not appreciably affect the observed prevalence of polarization Balmer jumps, as 17 of 40 (43%) exhibited such a signature. In contrast, the prevalence of polarization Balmer jumps does seem to be noticeably lower for later-type (B6-A0) Be stars, as we found only 8 of 26 (31%) exhibited evidence of a polarimetric Balmer jump.

The frequency of polarization Balmer jumps appears to decrease with metallicity: ~45% of Galactic Be stars in the HPOL database, ~25% of LMC Be stars from the present study, and ~4% of SMC Be stars from the present study exhibit polarization Balmer jumps. We suggest several possible explanations for these results.

1. It is possible that the average disk properties of classical Be stars are fundamentally different in the low metallicity environments of the SMC and LMC as compared to our Galaxy. The presence of intrinsic polarization in classical Be stars, as well as its wavelength dependence, is a function of disk inclination angle, disk density, and the effective temperature of disk material. Thus the observed lower frequency of polarization Balmer jumps in our data suggest either that it might be harder to form massive disk systems in low metallicity environments or that the average disk temperature is higher in these lower metallicity environments, hence decreasing the amount of pre- and post-scattering absorption by neutral H I.

2. Our polarimetric observations provided a one time sampling of LMC and SMC candidate Be stars, while the HPOL survey obtained a larger number of observations, albeit at quasi-random intervals, of a population of known Be stars. Owing to the variable nature of the Be phenomenon, we do not a priori know how often any individual Be star will exhibit any of the possible polarization signatures; hence, the different sampling errors associated with these two databases might explain at least some of the observed differences in the polarization Balmer jump frequencies.

3. The statistics presented in Table 11 were based on removing a significant number of objects deemed unlikely to be classical Be stars from consideration, i.e. type-3 and type-4 objects. Recall however that our definition of type-2 objects only required their polarimetric properties to be not inconsistent

with those expected from classical Be stars. It is possible that a population of "contaminants", either a) unpolarized objects which aren't pole-on or near pole-on classical Be stars; or b) non-classical Be stars which were not identified as such due to low data quality, still reside within our collection of type-2 objects, hence underestimate our polarization Balmer jump fraction frequency. If such a scenario is true, it would further suggest that extreme caution should be exercised when assessing the nature of stellar populations purely via the use of photometric 2-CDs.

5.2. *Identification of "Contaminants" in 2-CD Detected Candidate Be Stars*

WB06 identified a large number of B-type objects having excess Hα emission via photometric 2-CDs and suggested that these stars be classified as candidate Be stars. D. Gies (2006, personal communication) noted that several candidate Be stars in the WB06 dataset had colors redder than that expected from classical Be stars, and suggested that the frequency of observed blue (or red) excess Hα emitters in the 2-color diagrams presented in WB06 increased with the total number of stars of a given color range. Furthermore, he postulated that if these red excess emitters were a) a manifestation of extremely young stars with their birth disks still intact, b) red-type giants or supergiants, or c) false detections owing from the effects of bright background H II emission; measuring the prevalence of these excess emitters could serve as an estimate of the number of "contaminants" which affect the blue population of excess Hα emitters, i.e. the candidate Be star population.

We examined the 2-CD photometry of 6 clusters, common to both this survey and that of WB06 and spanning a wide range of ages (very young, young, old; WB06) and metallicities (SMC, LMC), and determined the frequency of excess red-type Hα emitters relative to the total number of red-type stars. We restricted our analysis such that the magnitude of (B-V) colors used to identify candidate Be stars in each cluster (i.e. $\sim$ -0.3 $<$ (B-V) $<$ 0.2 in NGC 458, WB06) matched the range of (B-V) colors used to study the frequency of red-type excess emitters (i.e. 0.2 $<$ (B-V) $<$ 0.7 for NGC 458). Furthermore, we adopted the same (R-Hα) cutoffs delineating excess emitters from normal stars for each cluster as used by WB06. The results of this exercise are tabulated in column 2 of Table 12. Interestingly, with few exceptions, the frequency of potential "contaminants" implied by this technique is generally consistent with the minimum rate of contamination derived from our polarization results (see column 3 of Table 12, column 6 of Table 9), i.e. the candidates we assigned a Type 4 classification. Clearly this photometric contamination check can not provide a diagnostic on the Be classification of individual objects, unlike our polarimetry; however, we suggest that this technique might provide a rough estimate of the role of contaminants in cases in which detailed follow-up observations have not been made or are unfeasible.

5.3. *Be Stars in Very Young Clusters*

One of the interesting results presented in WB06 was the identification of candidate Be star in clusters of age 5-8 Myr, in an abundance similar to the general frequency of the Be phenomenon in our Galaxy, $\sim$17%. However, it was uncertain based on those results whether the detected excess Hα emitters a) were true classical Be star-disk systems; b) were B-type objects which still possessed remnant star-formation disks; or c) merely had diffuse Hα nebulosity coincidentally associated with them. Our intrinsic polarimetric dataset affords us the opportunity to explore these issues in detail for 4 of these very young clusters, LH 72, NGC 1858, NGC 346, and NGC 371.

Tables 8, 10, and 11 all indicate that a significant number of objects in these very young clusters exhibit either electron scattering or Balmer jump polarization features, which are the expected signatures of classical Be stars. Such signatures are only produced when the electron scattering optical depth is $\sim$1.0, i.e., that present in the innermost disk region of classical Be stars: the density of any coincident diffuse Hα nebulosity present around candidates is vastly insufficient to create such a polarization signature. Thus while some of the "Be star" detections made by Hα spectroscopic surveys (Mazzali et al. 1996) have been shown to be spurious detections due to the presence of coincident gas (Keller & Bessell 1998), such diffuse nebulosity can not be responsible for creating the polarimetric signals found in our dataset.

Hillenbrand et al. (1993) discuss the stellar population of the young (2 Myr) cluster NGC 6611 and suggest that some of its members retain remnant gas disks from the star formation process. Could such disks also be prevalent in our sample of clusters of age 5-8 Myr? The candidates in our very young clusters do not have abnormal colors (see e.g. color magnitude diagrams in WB06), thus they likely do not have large star-formation dust disks. The observed intrinsic polarization signatures require that these disk systems, whether they are remnant star-formation disks or classical Be circumstellar disks, not be oriented near pole-on. This geometry requirement also limits the amount of dust which could be present in these systems, as we must be able to see through any such component in order to detect the gas disks present. Therefore, if these candidates did have remnant star formation disks, these systems must have already begun the disk dissipation process. The current star formation paradigm suggests that the clearing of star-formation disks is an "inside-out" process; thus, if our candidates had remnant star formation disks, the denser, inner regions of these disks would have already been cleared out. However, recall that the electron scattering and Balmer jump intrinsic polarization signatures requires a sufficient electron scattering optical depth in the inner disk region. Our intrinsic polarization observations thus rule out the possibility that our candidates have significant remnant gas disks from the star formation process.

5.3.1. *Be Stars in the First Half of a B Star's Main Sequence Lifetime: A Comparison to Fabregat & Torrejon (2000) and Martayan et al. (2006)*

Having ruled out alternative scenarios, our present dataset has confirmed the suggestion of WB06 that bonafide classical Be stars do develop before the mid-point main

sequence lifetime of a B star. Specifically, we have confirmed the presence of a significant number of bona-fide classical Be stars, having crude photometric spectral types of B0-B5 (WB06), in clusters spanning a near-continuous range of ages from log(t) of 6.7-8.1, i.e. 5-126 Myr. This directly refutes claims made by Fabregat & Torrejon (2000) and Martayan et al. (2006) that the Be phenomenon develops in the second-half of a B star's main sequence lifetime. Martayan et al. (2006) suggest that massive Be stars may briefly appear near the ZAMS in the SMC and LMC, before losing their "Be status" until the very end of the first part of their main sequence lifetimes, although this elaborate claim might in fact represent an overinerpretation of their dataset, which was essentially based on a single cluster population. The validity of this scenario as outlined by Martayan et al. (2006) is also doubtful in light of the results of WB06 and the present dataset. WB06 identified a large body of candidate Magellanic Cloud Be stars, having crude photometrically-assigned spectral types of B0-B5, in clusters spanning a range of ages from 5-126 Myr; no abrupt absence of classical Be stars was observed in any of the younger-type clusters. The present study has confirmed the Be status of many of the B0-B3 type candidate Be stars in clusters spanning a range of ages from 5-126 Myr; no abrupt absence of classical Be stars was observed in any of the younger-type clusters. Thus, our larger, more complete investigation of Be stars in Magellanic Cloud clusters reveals only evidence which contradicts the evolutionary scenario outlined by Martayan et al. (2006).

5.3.2. *Implications of the Presence of Be Stars in Very Young Clusters*

WB06 first reported the presence of candidate classical Be stars in clusters as young as 5 Myr, and noted that if such objects were truly classical Be stars, they would not have spent enough time on the main sequence to spin-up to near-critical rotation velocities via the mechanism proposed by Meynet & Maeder (2000) or via mass transfer in a binary system (McSwain & Gies 2005). Our present work has confirmed that bona-fide classical Be stars do reside in clusters as young as 5 Myr. We suggest that this is evidence that a significant number of classical Be stars might emerge onto the zero-age-main-sequence at near critical rotation velocities. An alternative interpretation of our results does not invoke having a significant population of stars emerge onto the ZAMS as near-critical rotators; rather, it is possible that these youthful bona-fide classical Be stars are evidence of the existence of a subset of the Be phenomenon which rotate at significantly sub-critical rates, perhaps as low as 0.4-0.6 v_{crit} for early-type B stars (Cranmer 2005). Cranmer (2005) suggest that only a subset of early-type (O7-B2) Be stars might be sub-critical rotators, while later-type objects (B3-A0) should be all near-critical rotators. Our photometric survey of these very young clusters assigned crude spectral types to these candidate Be stars of B0-B5 (WB06); however, owing to detection biases in our follow-up polarimetric observations, we have in general only been able to confirm that portions of the brightest of these candidates (i.e. the earliest spectral sub-types, B0 to ~B3) are bona-fide classical Be stars. Thus our present observations do not rule out the possibility that some of our very young bona-fide classical Be stars might belong to the sub-critical rotation population predicted by, e.g. Cranmer (2005).

The observed emergence of the Be phenomenon earlier in the main sequence lifetime than previously thought also has important implications regarding the role of magnetic fields in the formation of Be disks (Cassinelli et al. 2003). MacGregor & Cassinelli (2003) investigated the transport of magnetic flux tubes in 9 M_{sun} stars (~B2.5-B3) and found these structures could rise from the core to the surface within the (at the time) expected beginning of the Be phenomenon, the mid-point main sequence lifetime. The present study has confirmed the presence of bona-fide classical Be stars in clusters as young as 5 Myr having crude, photometrically assigned spectral types of B0 to ~B3. Although WB06 suggested the presence of an additional population of B4-B5 type candidate Be stars in these clusters, the limited dynamical range probed by the present study was unable to confirm the status of these fainter candidates. Although the magnetic flux transport model of MacGregor & Cassinelli (2003) had sufficient time to transport flux to the stellar surface for ~B3 stars, this is unlikely to be the case for later type stars ($\geq$B4) which have a much thicker radiative envelope. Hence, the existence of such later-type Be stars in extremely young clusters would likely require an additional mechanism to be employed to accelerate the rise times of magnetic flux (Cassinelli, 2006 personal communication). While challenging, follow-up spectroscopy of these young cluster populations would provide one avenue confirm the presence of these purported (Wisniewski & Bjorkman 2006) later-type systems.

5.4. *Future Work*

While the present study made significant advances in identifying and understanding the biases present in earlier 2-CD studies of cluster populations, additional work is clearly required. Our polarimetric survey was not sensitive to pole-on or near-pole-on systems, hence determining which of our "type-2" objects are near-pole-on classical Be stars and which are astrophysical objects of a fundamentally different nature is a high priority. We suggest that followup moderate resolution optical spectroscopic or infrared photometric observations would provide reasonable diagnostics to resolve this bias, and enable more quantitative determinations of the bona-fide classical Be content of clusters as a function of age and/or metallicity. Our data suggest that at least 25% of photometrically identified candidate Be stars appear unlikely to be true classical Be stars; however, we are unable to place firm constraints on the true astrophysical nature of such objects. We suggest that followup infrared photometric and/or spectroscopic observations would be useful to further constrain the evolutionary nature of these objects. Furthermore, such observations would also be useful to ascertain the true nature of candidate Be stars which were too faint to be reliably probed by our polarimetric observations.

Our analysis of the intrinsic polarization properties of LMC and SMC classical Be stars suggests that the fundamental disk properties of classical Be stars may depend on metallicity. Modeling followup moderate resolution spectropolarimetric observations of LMC/SMC classical Be

stars is a clear avenue one could use to further investigate these results, and we note that the advent of accurate linear spectropolarimeters on large aperture telescopes (i.e. the Focal Reducer Spectrograph (FORS) at the Very Large Telescope (VLT) or the Robert Stobie Spectrograph at the South African Large Telescope (SALT)) make obtaining such observations feasible.

6. SUMMARY

We have used photo-polarimetric observations of six LMC and six SMC clusters to investigate the true nature of their candidate Be populations, which were initially identified via 2-color diagram photometric techniques. The interstellar polarization components of these data were first identified in a systematic manner, allowing us to isolate the intrinsic polarization properties of our data. The interstellar polarization associated with NGC 330 appeared to be characterized by a λ_{max} value of $\sim$4500Å, suggesting the presence of a small dust grain population; furthermore, the ISP of NGC 2100 exhibited strong evidence of a complex morphology, which we will explore in a later paper.

Our intrinsic polarization offered definitive proof that clusters of age 5-8 Myr have a non-negligible population of bona-fide classical Be stars, clearly refuting suggestions that the Be phenomenon only develops in the second half of a B star's main sequence lifetime (Fabregat & Torrejon 2000; Martayan et al. 2006), i.e. after 10 Myr. We believe the most likely implication of these results is that a significant population of stars must emerge onto the ZAMS rotating at near critical velocities, although we note that these results do not exclude the possibility we are observing the hypothesized subset of classical Be stars which rotate at sub-critical velocities (Cranmer 2005).

Comparing the polarimetric properties of our dataset to a similar survey of Galactic classical Be stars, we find the prevalence of polarimetric Balmer jump signatures decreases with metallicity. We speculate that these results might indicate that either it is more difficult to form large disk systems in low metallicity environments, or that the average disk temperature is higher in these low metallicity environments.

We also found evidence that at least 25% of photometrically identified candidate Be stars do not exhibit polarimetric signatures consistent with those expected from classical Be stars. These data strongly suggest that caution must be exercised when attempting to correlate the onset of the Be phenomenon with evolutionary age and/or metallicity based solely on statistics derived from simple 2-color diagram photometry.

We thank Joe Cassinelli and Doug Gies for discussions which enhanced several aspects of this paper. The efforts of Brian Babler, Ken Nordsieck, and the PBO observing crew for supplying the HPOL data presented here are greatly appreciated. We thank the NOAO TAC for allocating observing time for this project and JPW thanks NOAO for supporting his travel to CTIO. Portions of this work has been supported in part by NASA GRSP NGT5-50469 (JPW), NASA LTSA NAG5-8054 (KSB), and NSF AST-0307686 (JEB) grants. AMM acknowledges travel support by FAPESP; he is also partially supported by CNPq. Polarimetry at the University of São Paulo (USP) is supported by FAPESP. This research has made use of the SIMBAD database operated at CDS, Strasbourg, France, and the NASA ADS system.

REFERENCES

Bjorkman, K.S. 1994, Ap&SS, 221, 335
Bjorkman, K.S. 2000, in IAU Coll. 175 "The Be Phenomenon in Early-Type Stars", ed. M. Smith & H. Henrichs (ASP: San Francisco) 214, 384
Bjorkman, K.S., Meade, M.R., & Babler, B.L. 2000, in IAU Coll. 175 "The Be Phenomenon in Early-Type Stars", ed. M. Smith & H. Henrichs (ASP: San Francisco) 214, 48
Cassinelli, J.P., Brown, J.C., Mahesaran, M., Miller, N.A., & Telfer, D.C. 2003, ApJ, 578, 951
Clarke, D.S. & Bjorkman, K.S. 1998, A&A, 331, 1059
Clayton, G.C., Martin, P.G., & Thompson, I. 1983, ApJ, 265, 194
Coyne, G.V. & Kruszewski, A. 1969, AJ, 74, 528
Coyne, G.V. & McLean, I.S. 1982, in Be Stars, IAU Symp No. 98, eds. M. Jaschek & H.-G. Groth, Reidel, Dordrecht, 77
Cranmer, S.R. 2005, ApJ, 634, 585
Dieball, A. & Grebel, E.K. 1998, A&A, 339, 773
Fabregat, J. & Torrejon, J.M. 2000, A&A, 357, 451
Feast, M.W. 1972, MNRAS, 159, 113
Grebel, E.K., Richtler, T., & de Boer, K.S. 1992, A&A, 254, L5
Grebel, E.K. 1997, A&A, 317, 448
Grebel, E.K. & Chu, Y. 2000, AJ, 119, 787
Hillenbrand, L.A., Massey, P., Strom, S.E., & Merrill, K.M. 1993, AJ, 106, 1906
Keller, S.C. & Bessell, M.S. 1998, A&A, 340, 397
Keller, S.C., Wood, P.R., & Bessell, M.S. 1999, A&AS, 134, 489
Keller, S.C., Bessell, M.S., & Da Costa, G.S. 2000, AJ, 119, 1748
Keller, S.C. 2004, PASA, 21, 310
Maeder, A., Grebel, E.K., & Mermilliod, J-C. 1999, A&A, 346, 459
MacGregor, K.B. & Cassinelli, J.P. 2003, ApJ, 586, 480
Magalhães, A.M. 1992, ApJ, 398, 286
Magalhães, A.M., Rodrigues, C.V., Margoniner, V.E., & Pereyra, A. 1996, in ASP Conf. Ser. 97, Polarimetry of the Interstellar Medium, ed. W.G. Roberge & D.C.B. Whittet (San Francisco:ASP), 118
Martayan, C., Fremat, Y., Hubert, A.-M., Floquet, M., Zorec, J., & Neiner, C. 2006, A&A, in press
Mazzali, P.A., Lennon, D.J., Pasian, F., Marconi, G., Baade, D., & Castellani, V. 1996, A&A, 316, 173
McDavid, D. 1994, PASP, 106, 949
McLean, I.S. & Brown, J.C. 1978, A&A, 69, 291
McSwain, M.V. & Gies, D.R. 2005, ApJS, 161, 118
Melgarejo, R., Magalhães, A.M., Carciofi, A.C., & Rodrigues, C.V., 2001, A&A, 377, 581
Mermilliod, J.-C. 1982, A&A, 109, 48
Meynet, G. & Maeder, A. 2000, A&A, 361, 101
Olsen, K.A.G., Kim, S., & Buss, J.F. 2001 , AJ, 121, 3075
Pereyra, A. 2000, Ph.D. thesis, Univ. of São Paulo
Pereyra, A. & Magalhães, A.M. 2002, ApJS, 141, 469
Poeckert, R. & Marlborough, J.M. 1976, ApJ, 206, 182
Porter, J.M. 1996, MNRAS, 280, 31
Porter, J.M. & Rivinius, T. 2003, PASP, 115, 1153
Quirrenbach, A. et al. 1997, ApJ, 479, 477
Rodrigues, C.V., Magalhães, A.M., Coyne, G.V., & Piirola, S.J.V. 1997, ApJ, 485, 618
Schmidt, Th. 1976, A&AS, 24, 357
Schmidt, G.D., Elston, R., & Lupie, O.L. 1992, AJ, 104, 1563
Schulte-Ladbeck, R.E. et al. 1992, ApJL, 401, 105
Serkowski, K., Mathewson, D.S., & Ford, V.L. 1975, ApJ, 196, 261
Struve, O. 1931, ApJ, 73, 94
Whittet, D.C.B., Martin, P.G., Hough, J.H., Roush, M.F., Bailey, J.A., & Axon, D.J. 1992, ApJ, 386, 562
Wilking, B.A., Lebofsky, M.J., & Rieke, G.H. 1982, AJ, 87, 695
Wisniewski, J.P., Bjorkman, K.S., & Magalhães, A.M. 2003, ApJL, 598, 43
Wisniewski, J.P. & Bjorkman, K.S. 2006, ApJ, in press (WB06)
Wisniewski, J.P., Bjorkman, K.S., Magalhães, A.M., & Pereyra, A. 2006, ApJ, in prep
Wolff, M.J., Nordsieck, K.H., & Nook, M.A. 1996, AJ, 111, 856
Wood, K. & Bjorkman, J.E. 1995, ApJ, 443, 348
Wood, K., Bjorkman, K.S., & Bjorkman, J.E. 1997, ApJ, 477, 926

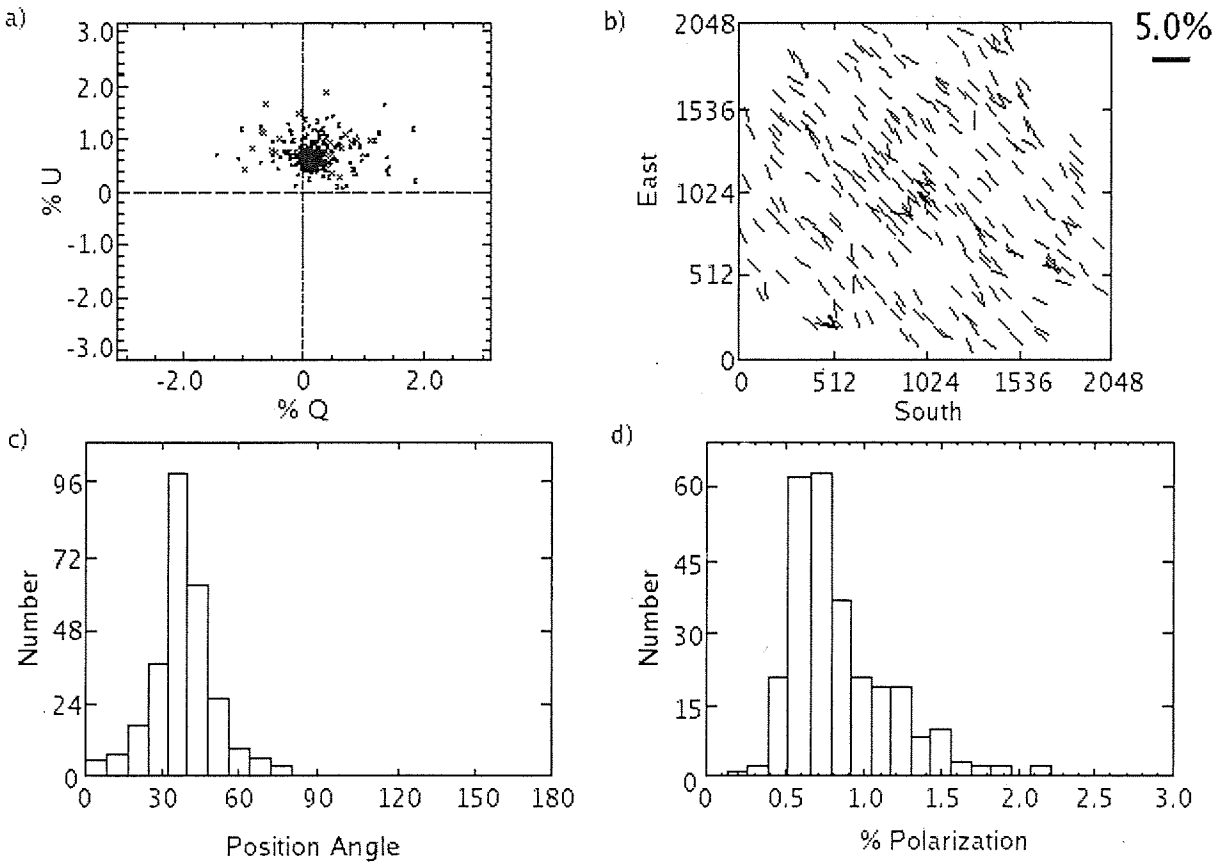

FIG. 1.— The output of the PCCDPACK routine *select* for the V-band observation of NGC 1818 is shown. Cluster members having a polarimetric signal-to-noise level, p/σ_p, greater than 5 are plotted on a Stokes Q-U diagram (panel a), as a polarization map as a function of pixel location (panel b), and in position angle (panel c) and polarization (panel d) histograms. As many cluster stars in panels a, c, and d exhibit the same general polarimetric properties, we suggest that most of these objects lack significant intrinsic polarization components and instead only exhibit evidence of interstellar polarization.

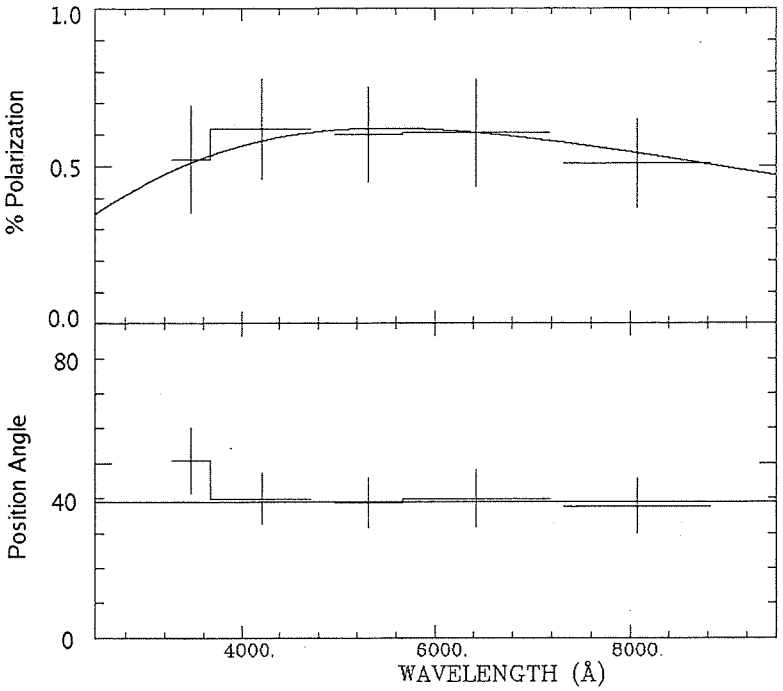

FIG. 2.— The observationally derived total ISP estimates for each filter of NGC 1818 are plotted as a function of wavelength. The data closely follow a classic Serkowski-law shape (Serkowski et al. 1975), suggesting that our method for determining the ISP in each cluster was reasonable. Over-plotted on these estimates is a modified Serkowski-law (Serkowski et al. 1975; Wilking et al. 1982) which we deemed best fit the estimates. We extracted the U, B, V, R, and I filter polarization associated with this fit, and hereafter use these values to describe the ISP of NGC 1818.

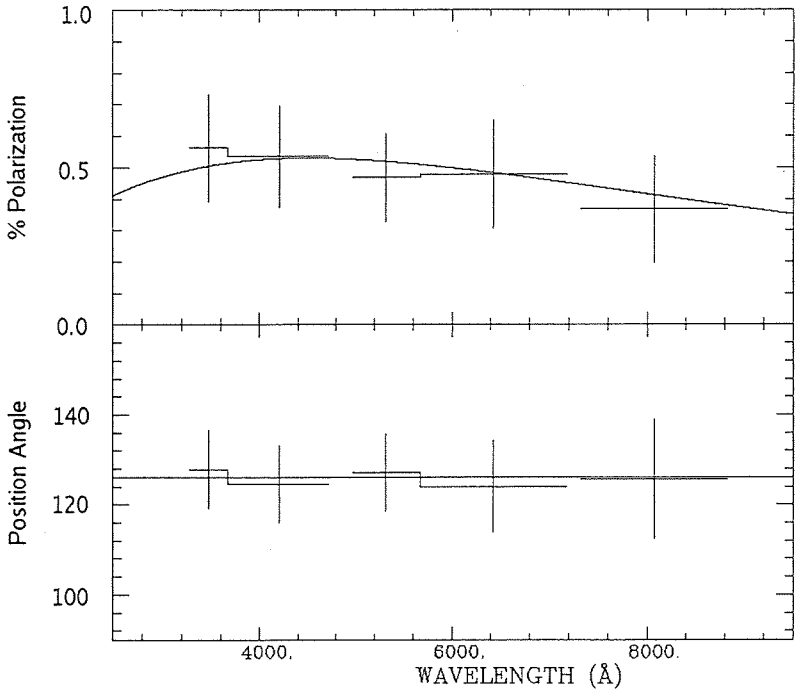

FIG. 3.— The observationally derived total ISP estimates for each filter of NGC 330 are plotted as a function of wavelength. Over-plotted on these estimates is a modified Serkowski-law (Serkowski et al. 1975; Wilking et al. 1982) which we deemed best fit the data. These data, as well as the SMC ISP associated with NGC 330 (see Table 4) are characterized by a λ_{max} value of $\sim$4500 Å, suggesting the presence of smaller than average dust grains.

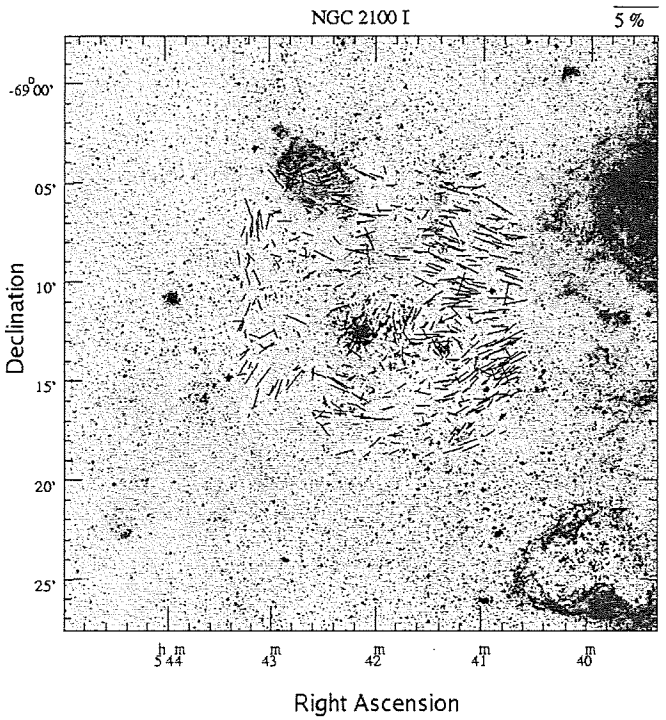

FIG. 4.— The total polarization vectors of our observations of the LMC cluster NGC 2100 are over-plotted on a DSS-2 red image. The general morphology of these polarization vectors matches that seen in the other 4 filters observed, indicating this structure is real.

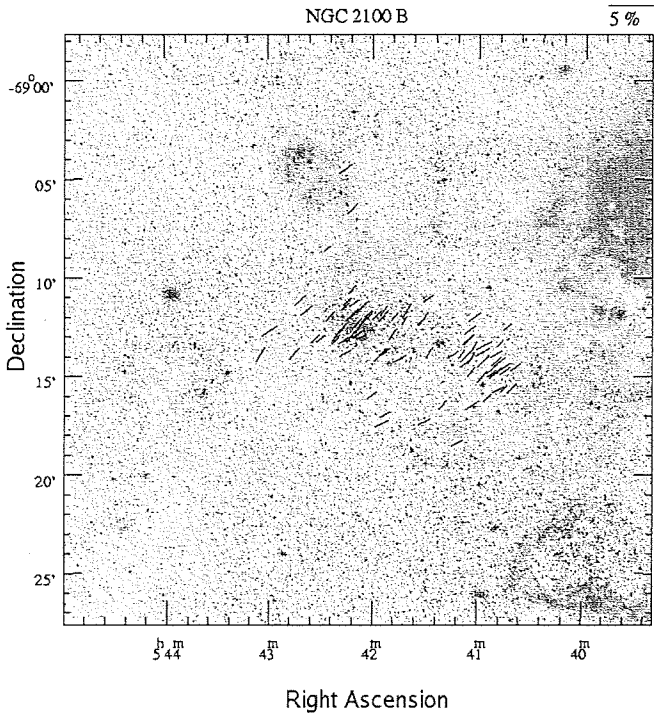

FIG. 5.— The B-band polarization vector map of region 1 in NGC 2100 ISP space is over-plotted on a DSS-2 blue image.

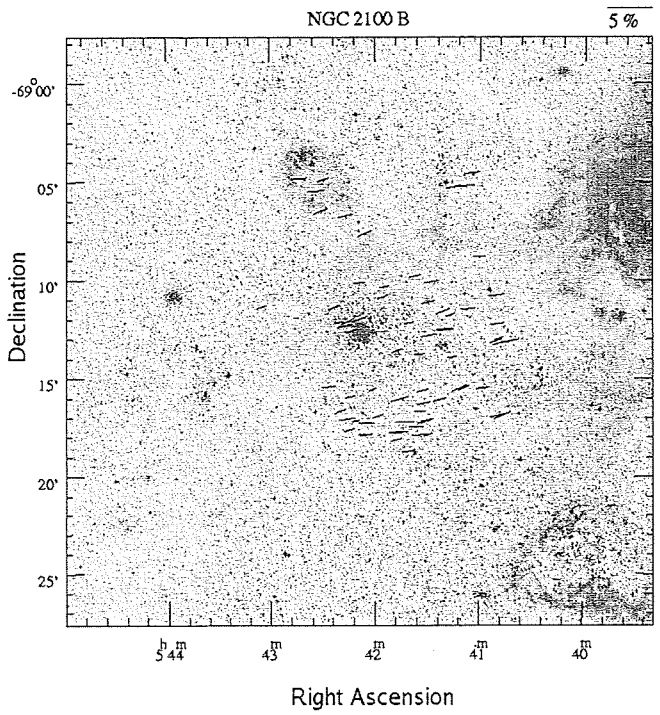

FIG. 6.— The B-band polarization vector map of region 2 in NGC 2100 ISP space is over-plotted on a DSS-2 blue image.

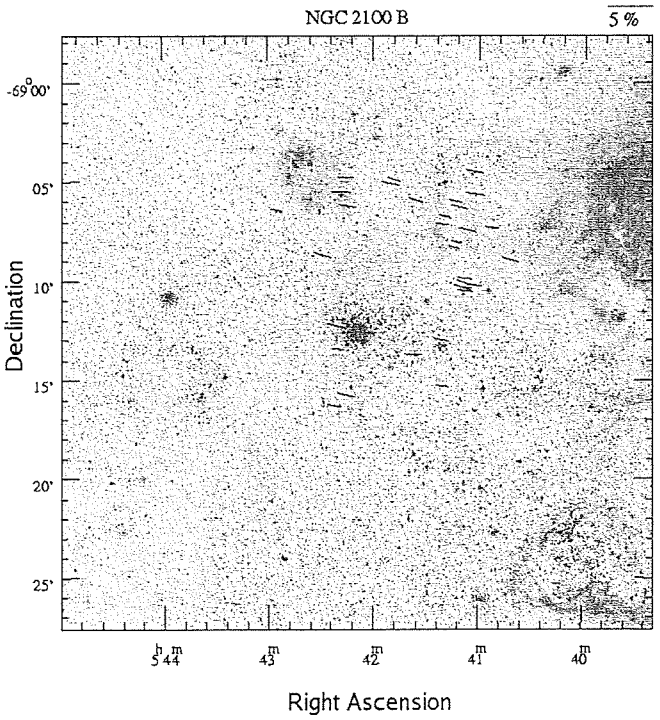

FIG. 7.— The B-band polarization vector map of region 3 in NGC 2100 ISP space is over-plotted on a DSS-2 blue image.

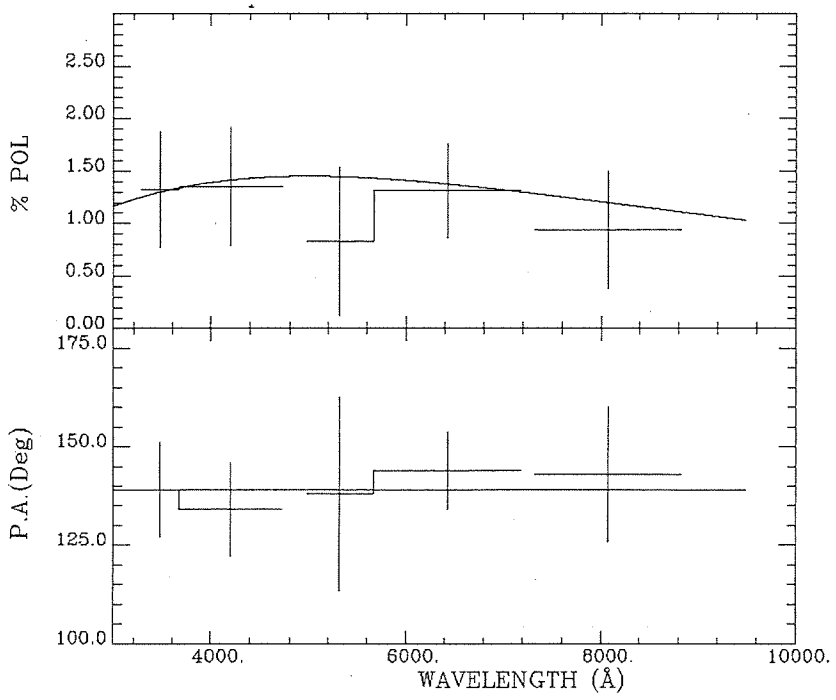

FIG. 8.— The observationally derived initial estimates of the total interstellar polarization towards region 1 of NGC 2100 is shown, along with the modified Serkowski-law we deemed best fit the data. The final ISP values for region 1 used in the remainder of this paper were extracted from this Serkowski curve.

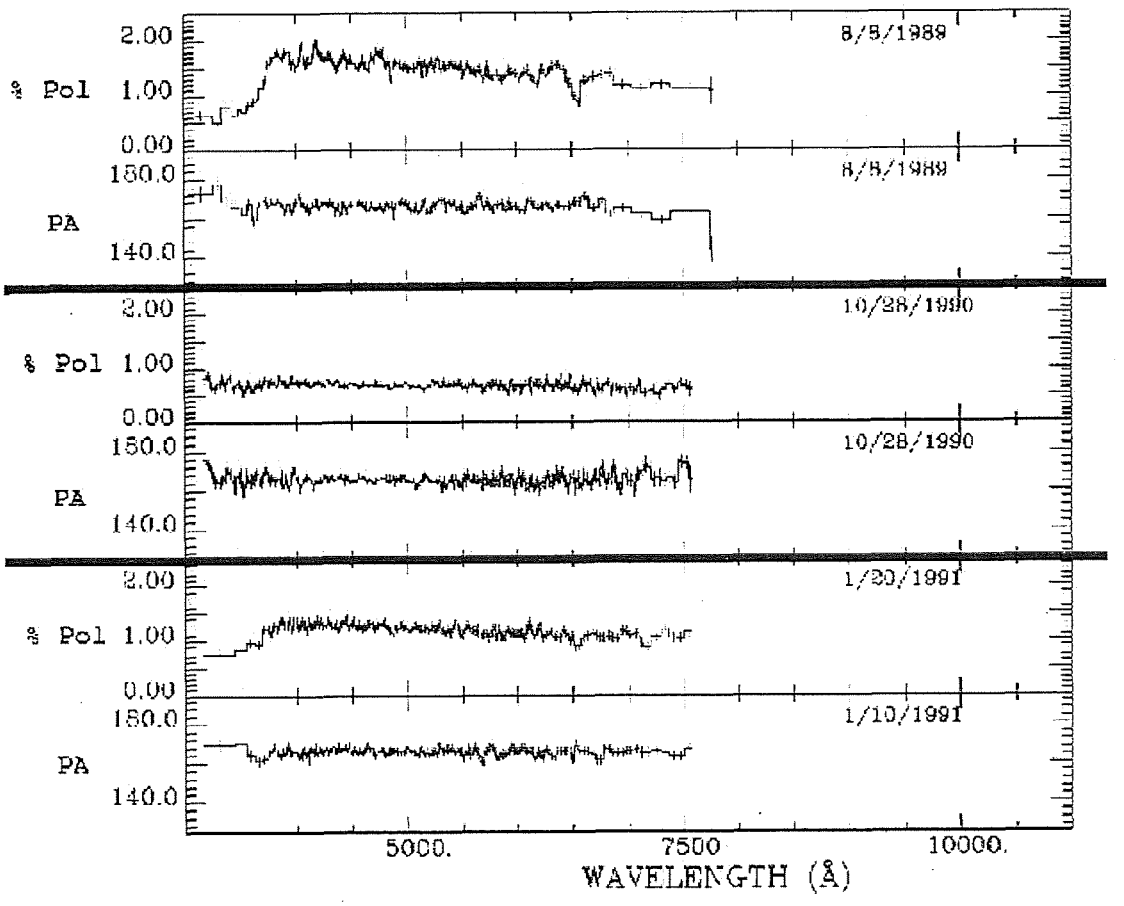

FIG. 9.— The time variability of the intrinsic polarization of the known Galactic classical Be star pi Aquarii is shown in these multi-epoch data from the HPOL spectropolarimeter. During the 1989 and 1991 observations, the inner disk density was sufficiently high such that the effects of pre- and post-scattering absorption by hydrogen in the disk is seen in the appearance of a polarization Balmer jump and a "saw-tooth" like wavelength dependence. The inner disk density was sufficiently low in the 1990 observation such that the wavelength independent electron scattering signature was not noticeably altered by a hydrogen opacity signature. We have examined our intrinsic imaging polarization observations of candidate Be stars to search for the polarimetric signatures found in this figure.

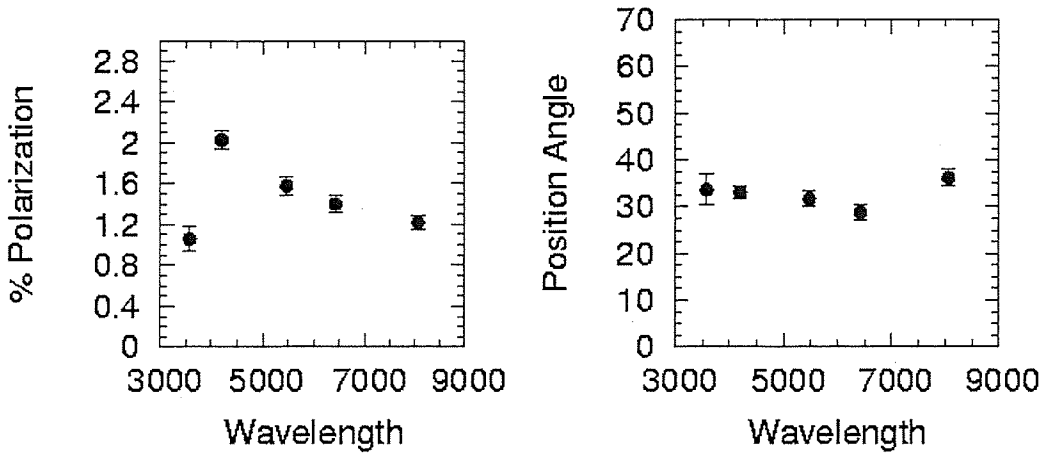

FIG. 10.— The intrinsic polarization of NGC 371:WBBe18 exhibits the "sawtooth-like" polarization signature characteristic of classical Be stars. Such objects were assigned a designation of type-1 to indicate they are definitely classical Be stars.

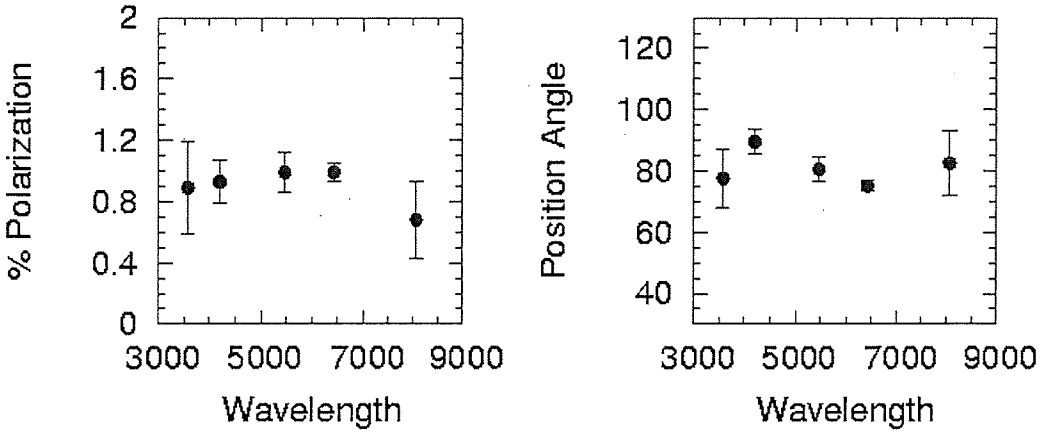

FIG. 11.— The intrinsic polarization of NGC 371:WBBe21 clearly exhibits a wavelength independent electron scattering polarization signature. Such objects were assigned a designation of type-2 to indicate they are not inconsistent with being classical Be stars.

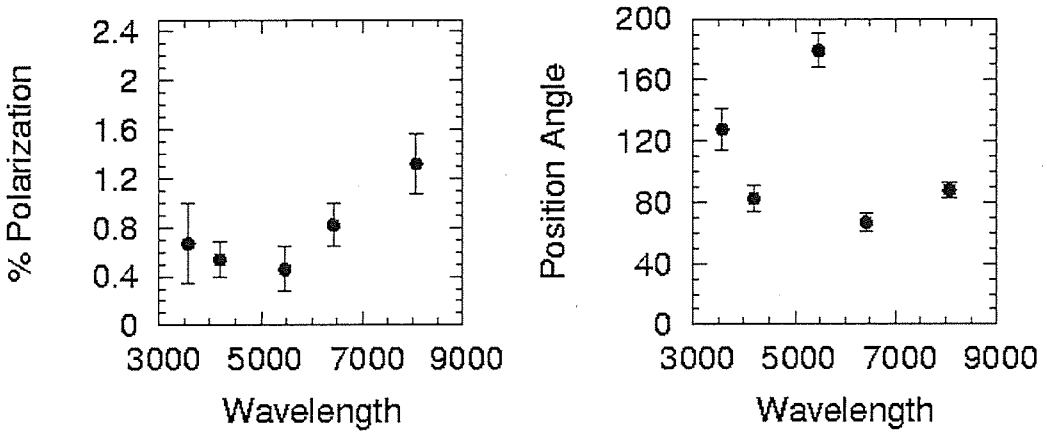

FIG. 12.— The intrinsic polarization of NGC 371:WBBe47 is not consistent, to within 3 σ, with that expected from a classical Be star. Such objects would receive a designation of type-3 or type-4, depending on the severity of their deviation from any of the expected polarimetric signatures. These objects (especially those which receive a type-4 designation) provide strong evidence that the 2-CD technique can mis-identify classical Be star-disk systems.

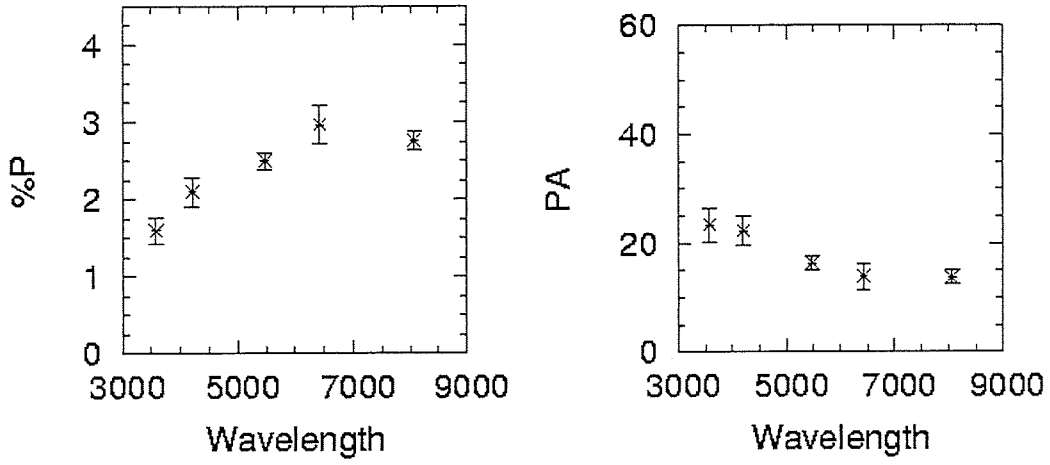

FIG. 13.— The intrinsic polarization of NGC 1948:KWBBe 246 follows a complex wavelength dependence. The optical polarization appears to decrease and position angle increase at short wavelengths. Objects which have dusty plus gaseous disks, such as HD 45677 (Schulte-Ladbeck et al. 1992), exhibit similar optical polarimetric behavior, suggesting that NGC 1948:KWBBe 246 and similar objects in our sample might also be characterized by such disks. Alternatively, the wavelength dependence of these data also resemble a Serkowski-like behavior (Serkowski et al. 1975), which as discussed in Section 4 might indicate that some these types of objects are characterized by abnormal interstellar dust conditions.

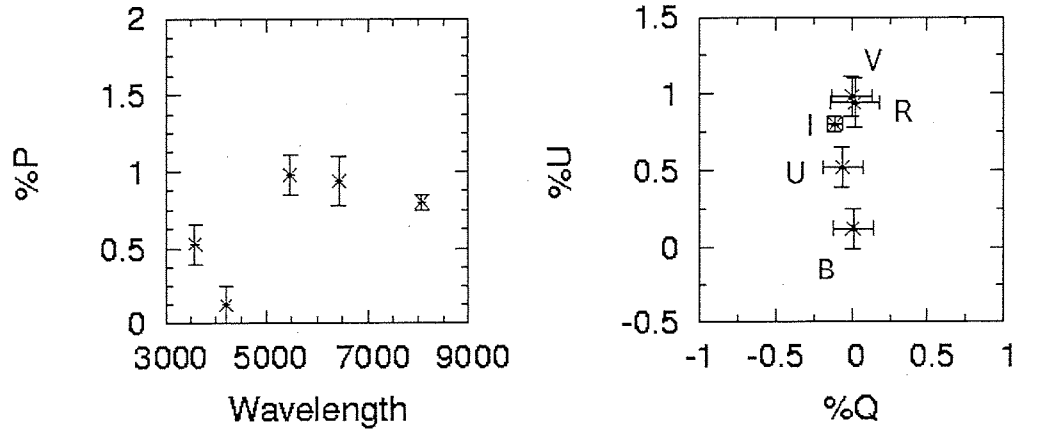

FIG. 14.— The wavelength dependent intrinsic polarization of NGC 2100:KWBBe 111 clearly is not consistent with that expected from a classical Be star. We suggest that this object might be a dust-disk system.

TABLE 1

SUMMARY OF OUR OBSERVATIONS

Cluster	Location	Filter	Age	Date	Exposure Time
Bruck 60	SMC	U	o	2002 Oct 19	1200
...	...	B	...	2002 Oct 21	720
...	...	V	...	2002 Oct 19	300
...	...	R	...	2002 Oct 19	300
...	...	I	...	2002 Oct 21	300
NGC 330	SMC	U	y	2001 Nov 22	1200
...	...	B	...	2001 Nov 23	420
...	...	V	...	2001 Nov 25	300
...	...	R	...	2001 Nov 25	240
...	...	I	...	2001 Nov 24	240
NGC346	SMC	U	vy	2001 Nov 21	720
...	...	B	...	2001 Nov 22	240
...	...	V	...	2001 Nov 21	180
...	...	R	...	2001 Nov 24	180
...	...	I	...	2001 Nov 23	180
NGC 371	SMC	U	vy	2002 Oct 18	1200
...	...	B	...	2002 Oct 18	600
...	...	V	...	2002 Oct 17	420
...	...	R	...	2002 Oct 17	300
...	...	I	...	2002 Oct 18	420
NGC 456	SMC	U	y	2002 Oct 24	1200
...	...	B	...	2002 Oct 26	720
...	...	V	...	2002 Oct 24	420
...	...	R	...	2002 Oct 26	300
...	...	I	...	2002 Oct 25	300
NGC 458	SMC	U	o	2002 Oct 27	1200
...	...	B	...	2002 Oct 27	720
...	...	V	...	2002 Oct 26	300
...	...	I	...	2002 Oct 27	300
LH 72	LMC	U	vy	2002 Oct 26	1200
...	...	B	...	2002 Oct 25	720
...	...	V	...	2002 Oct 25	420
...	...	R	...	2002 Oct 27	360
...	...	I	...	2002 Oct 26	300
NGC 1818	LMC	U	y	2001 Nov 21	900
...	...	B	...	2001 Nov 22	240
...	...	V	...	2001 Nov 21	240
...	...	R	...	2001 Nov 22	180
...	...	I	...	2001 Nov 22	300
NGC 1858	LMC	U	vy	2002 Oct 19	1200
...	...	B	...	2002 Oct 24	720
...	...	V	...	2002 Oct 18	420
...	...	R	...	2002 Oct 21	300
...	...	I	...	2002 Oct 24	300
NGC 1948	LMC	U	y	2001 Nov 27	1200
...	...	B	...	2001 Nov 26	360
...	...	V	...	2001 Nov 25	180
...	...	R	...	2001 Nov 26	240
...	...	I	...	2001 Nov 26	300
NGC 2004	LMC	U	y	2001 Nov 25	900
...	...	B	...	2001 Nov 22	180
...	...	V	...	2001 Nov 27	180
...	...	I	...	2001 Nov 22	420
NGC 2100	LMC	U	y	2001 Nov 24	1200
...	...	B	...	2001 Nov 23	240
...	...	V	...	2001 Nov 23	180
...	...	R	...	2001 Nov 24	180
...	...	I	...	2001 Nov 23	180

Note. — We summarize some of the properties of the data presented in this paper. The exposure times listed are the integration time used at each of eight wave-plate position. The age labels in column 4, originally defined and discussed in detail in Wisniewski & Bjorkman (2006), correspond to very young (vy) 5-8 Myr; young (y) 10-25 Myr; and old (o) 32-158 Myr.

TABLE 2

AVERAGE INTERSTELLAR POLARIZATION

Cluster	% P_u	% P_b	% P_v	% P_r	% P_i	PA	P_{max}	λ_{max}	dPA	K
Bruck 60	0.46±0.18%	0.51±0.30%	0.55±0.23%	0.54±0.19%	0.48±0.19%	130	0.55%	5500	0	0.923
LH 72	0.34±0.14%	0.37±0.12%	0.40±0.14%	0.39±0.12%	0.35±0.14%	28	0.40%	5500	0	0.923
NGC 330	0.51±0.17%	0.53±0.16%	0.52±0.14%	0.48±0.17%	0.41±0.17%	126	0.53%	4500	0	0.737
NGC 346	0.31±0.17%	0.35±0.18%	0.37±0.17%	0.36±0.15%	0.32±0.19%	125	0.37%	5500	0	0.923
NGC 371	0.38±0.15%	0.42±0.16%	0.45±0.15%	0.44±0.15%	0.39±0.15%	118	0.45%	5500	0	0.923
NGC 456	0.57±0.21%	0.63±0.24%	0.67±0.25%	0.66±0.29%	0.58%	147	0.67%	5500	-8	0.923
NGC 458	0.33±0.34%	0.36±0.23%	0.39±0.22%	···	0.34±0.15%	120	0.39%	5500	0	0.923
NGC 1818	0.52±0.17%	0.58±0.16%	0.62±0.15%	0.61±0.17%	0.54±0.14%	39	0.62%	5500	0	0.923
NGC 1858	0.32±0.21%	0.36±0.15%	0.38±0.16%	0.37±0.22%	0.33±0.17%	45	0.38%	5500	0	0.923
NGC 1948	0.57±0.19%	0.64±0.15%	0.68±0.18%	0.67±0.17%	0.59±0.17%	35	0.68%	5500	0	0.923
NGC 2004	0.32±0.12%	0.36±0.13%	0.38±0.15%	···	0.33±0.16%	26	0.38%	5500	0	0.923

Note. — The Serkowski parameters PA, P_{max}, λ_{max}, dPA, and K which best described each of our clusters are tabulated, along with the final ISP values in the U, B, V, R, and I filters. The horizontal line separates SMC clusters (above) from LMC clusters (below).

TABLE 3

FOREGROUND ISP CORRECTIONS

Schmidt Region	Polarization	Position Angle	Clusters
Region I	0.37 ± 0.15%	111	Bruck 60
Region II	0.27±0.15%	123	NGC 330, 346, 371
Region III	0.19±0.21%	110	NGC 456, 458
Region VI	0.64±0.19%	30	LH 72
Region VII	0.32±0.13%	29	NGC 1818,1858,1948
Region IX	0.40±0.13%	20	NGC 2004

Note. — We used the Galactic polarization maps of Schmidt (1976) as templates to identify and remove the foreground Galactic interstellar polarization contribution to each of our Magellanic Cloud lines of sight. Columns two and three represent the corrections applied to each of our lines of sight, listed in column four.

TABLE 4

ISP INTRINSIC TO THE MAGELLANIC CLOUDS

Cluster	P_u	PA_u	P_b	PA_b	P_v	PA_v	P_r	PA_r	P_i	PA_i
Bruck 60[1]	0.43±0.23%	132±15	0.45±0.34%	133±22	0.34±0.27%	151±23	0.41±0.24%	138±17	0.33±0.24%	144±21
LH 72[4]	0.27±0.24%	28±26	0.24±0.22%	27±26	0.24±0.24%	123±29	0.07±0.22%	18±90	0.07±0.24%	130±98
NGC 330[2]	0.48±0.23%	126±14	0.48±0.22%	126±13	0.25±0.21	129±24	0.34±0.23%	127±19	0.24±0.23%	128±28
NGC 346[2]	0.28±0.23%	125±24	0.30±0.23%	125±22	0.10±0.23%	130±66	0.22±0.21%	126±27	0.15±0.24%	127±46
NGC 371[2]	0.35±0.21%	118±17	0.37±0.22%	117±17	0.19±0.21%	111±32	0.31±0.21%	116±19	0.22±0.21%	114±27
NGC 456[3]	0.56±0.30%	148±15	0.62±0.32%	149±15	0.64±0.33%	155±15	0.64±0.36%	151±16	0.56%	153.2
NGC 458[3]	0.31±0.40%	121±37	0.32±0.31%	121±28	0.22±0.30%	129±39	0.23±0.26%	125±32	···	···
NGC 1818[5]	0.49±0.21%	40±12	0.52±0.21%	40±12	0.34±0.20%	49±17	0.46±0.21%	43±13	0.35±0.19%	45±16
NGC 1858[5]	0.29±0.25%	47±25	0.31±0.20%	48±19	0.20±0.21%	74±30	0.25±0.26%	55±30	0.19±0.21%	63±32
NGC 1948[5]	0.54±0.23%	35±12	0.58±0.20%	36±10	0.37±0.22%	40±17	0.51±0.21%	37±12	0.39±0.21%	38±15
NGC 2004[6]	0.28±0.18%	27±18	0.28±0.18%	28±18	0.08±0.20%	75±72	0.09±0.21%	44±67	···	···

Note. — We corrected the total measured ISP components of each of our clusters for the effects of foreground Galactic interstellar polarization, revealing the ISP components which arose from the dichroic absorption of light by dust grains located within the Magellanic Clouds. The horizontal line separates SMC clusters (above) from LMC clusters (below).

TABLE 5

TOTAL INTERSTELLAR POLARIZATION TOWARD NGC 2100

Cluster	% P_u	% P_b	% P_v	% P_r	% P_i	PA	P_{max}	λ_{max}	dPA	K
NGC 2100 area 1	1.32%	1.41%	1.44%	1.37%	1.20%	139	1.45%	5000	0	0.83
NGC 2100 area 2	1.26%	1.35%	1.37%	1.31%	1.14%	100	1.38%	5000	0	0.83
NGC 2100 area 3	1.64%	1.69%	1.65%	1.54%	1.32%	78	1.70%	4500	0	0.737

Note. — A summary of the total interstellar polarization values toward NGC 2100 for the 3 distinct spatial regions identified within the field of view of our NGC 2100 dataset.

TABLE 6

TOTAL POLARIZATION OF CANDIDATE BE STARS

Candidate Be Star	Filter	%P	PA	% Q	% U	% Err
Bruck 60:WBBe 1	u	1.75	107.3	-1.44	-0.99	0.61
	b	...	...	...	...	...
	v	1.33	113.7	-0.90	-0.98	0.30
	r	1.33	117.6	-0.76	-1.09	0.35
	i	...	...	...	...	...

Note. — The total polarization (i.e. interstellar plus intrinsic components) of one candidate Be star investigated in this study is tabulated. A table presenting results for our entire dataset is available in the electronic version of this Journal.

TABLE 7

INTRINSIC POLARIZATION OF CANDIDATE BE STARS

Candidate Be Star	Filter	%P	PA	% Q	% U	% Err
Bruck 60:WBBe 1	u	1.46	100.9	-1.36	-0.54	0.61
	b	...	...	...	...	...
	v	0.91	104.4	-0.80	-0.44	0.30
	r	0.88	110.0	-0.67	-0.56	0.35
	i	...	...	...	...	...

Note. — The intrinsic polarization of one candidate Be star investigated in this study is tabulated. A table presenting results for our entire dataset is available in the electronic version of this Journal.

TABLE 8

CLASSIFYING THE INTRINSIC POLARIZATION OF INDIVIDUAL CANDIDATE BE STARS

Name	Pol Balmer Jump?	PA	Classification	Comments
Bruck 60:WBBe 1	N	F2	2	moderate ES

Note. — The classification of the intrinsic polarization signature of one of the candidate Be stars investigated in this study is presented. Column 2 indicates whether a polarization Balmer jump was present in the data; the letters in column 3 indicate whether the polarization position angle was flat (F), linearly sloped (S), or randomly variable (V) while the numbers indicate the σ level of such characterizations; column 4 indicates the likelihood each object is a bona-fide classical Be star based on the 4 point classification scheme described in the text; and any relevant comments are listed in column 5. Note that a table presenting results for our entire dataset is available in the electronic version of this Journal.

TABLE 9

INTRINSIC POLARIZATION SUMMARY

Cluster ...	Detection Rate ...	# Pol. BJ (type-1)	# ES (type-2)	Not Inconsistent (type-2)	Unlikely (type-3,4)
Bruck 60	18/26 (69%)	1/18 (6%)	8/18 (44%)	11/18 (61%)	6/18 (33%)
NGC 330	41/76 (54%)	0/41 (0%)	9/41 (22%)	24/41 (59%)	17/41 (41%)
NGC 346	33/48 (69%)	8/33 (24%)	7/33 (21%)	22/33 (67%)	3/33 (9%)
NGC 371	73/129 (57%)	10/73 (14%)	6/73 (8%)	49/73 (67%)	14/73 (19%)
NGC 456	14/23 (61%)	0/14 (0%)	1/14 (7%)	9/14 (64%)	5/14 (36%)
NGC 458	10/30 (33%)	0/10 (0%)	0/10 (0%)	6/10 (60%)	4/10 (40%)
LH 72	34/50 (67%)	1/34 (3%)	5/34 (15%)	22/34 (65%)	11/34 (32%)
NGC 1818	18/40 (45%)	4/18 (22%)	5/18 (28%)	12/18 (67%)	2/18 (11%)
NGC 1858	27/39 (69%)	3/27 (11%)	2/27 (7%)	13/27 (48%)	11/27 (41%)
NGC 1948	22/27 (81%)	6/22 (27%)	6/22 (27%)	12/22 (55%)	4/22 (18%)
NGC 2004	43/67 (64%)	9/43 (21%)	10/43 (23%)	28/43 (65%)	6/43 (14%)
NGC 2100	35/61 (57%)	8/35 (23%)	16/35 (46%)	20/35 (57%)	7/35 (20%)

Note. — We summarize the statistics of our classification of the intrinsic polarization properties of our dataset. The detection rate column describes the number of candidates for which we were able to extract polarimetric information. The third column denotes the fraction of candidates which display polarimetric Balmer jumps (BJ): we consider these objects to be bona-fide classical Be stars. The fourth column describes the fraction of candidates which exhibit electron scattering (ES) signatures, i.e. moderate amounts of wavelength-independent polarization at a wavelength independent position angle. The fifth column describes candidates that, to within 3 σ, can not be ruled out as possible Be stars. The sixth column describes candidate Be stars whose intrinsic polarization does not agree, to within 3 σ, with that expected from classical Be stars. The horizontal line separates SMC clusters (above) from LMC clusters (below).

TABLE 10

AVERAGE INTRINSIC POLARIZATION PROPERTIES

Cluster	Mean BJ	Median BJ	Mean ES	Median ES	Mean Unlikely	Median Unlikely
Very Young	13%	13%	13%	12%	25%	26%
Young	13%	21%	22%	23%	26%	20%
SMC	7%	3%	17%	15%	30%	35%
LMC	18%	22%	24%	25%	23%	19%
ALL SMC+LMC	13%	13%	21%	22%	26%	26%

Note. — Statistical averages of data listed in Table 9 are presented. Clusters were grouped according to age (very young and young) as well as metallicity (SMC and LMC). The final entry labeled *ALL* denotes a global average of all SMC and LMC cluster data regardless of age or metallicity.

TABLE 11

AVERAGE INTRINSIC POLARIZATION PROPERTIES WITH "CONTAMINANTS" REMOVED

Cluster	Mean BJ	Median BJ	Mean ES	Median ES
Very Young	17%	18%	17%	18%
Young	16%	24%	28%	31%
SMC	7%	4%	25%	17%
LMC	22%	25%	31%	29%
ALL LMC+SMC	16%	18%	28%	25%
Milky Way Galaxy	42-49%	...	...	...

Note. — Objects deemed unlikely to be classical Be stars in Table 10 were removed from consideration, and the statistical averages of data listed in Table 9 were recalculated. The "ALL SMC+LMC" entry denotes a global average of all SMC and LMC cluster data regardless of age or metallicity. The Milky Way data averages were derived from analysis of the HPOL polarization catalog, as discussed in Section 5.1.

TABLE 12

FREQUENCY OF CONTAMINANTS IN BE POPULATIONS IDENTIFIED VIA 2-CDS

Cluster	Analysis of 2-CD data	Analysis of Polarimetry
Bruck 60	14%	33%
NGC 371	11%	19%
NGC 456	10%	36%
NGC 458	38%	40%
LH 72	25%	32%
NGC 1858	42%	41%

Note. — The possible rate of contamination of classical Be star detections extracted from photometric 2-color diagrams. As discussed in Section 5.2, the second column represents the frequency of red-type excess Hα emitters, which we suggest might be an appropriate proxy of the frequency of B-type excess Hα emitters which are not classical Be stars. The third column is a reproduction of column 6 in Table 9 and illustrates the frequency of 2-CD contaminants as derived from polarimetric observations of candidate Be stars.